Vol 18 No 6, June 2009
1674-1056/2009/18(06)/2271-11

Chinese Physics B

© 2009 Chin. Phys. Soc.
and IOP Publishing Ltd

Theoretical studies on the one- and two-photon absorption properties of azulenylporphyrins and azulene-fused porphyrins*

Li Wen-Chao(李文超)[a], Feng Ji-Kang(封继康)[a)b)†], Ren Ai-Min(任爱民)[a], Zhang Xiang-Biao(张祥标)[a], and Sun Chia-Chung(孙家钟)[a]

[a] *State Key Laboratory of Theoretical and Computational Chemistry, Institute of Theoretical Chemistry, Jilin University, Changchun* 130023, *China*

[b] *College of Chemistry, Jilin University, Changchun* 130023, *China*

(Received 16 December 2008; revised manuscript received 9 January 2009)

The electronic structures, one-photon absorption (OPA) and two-photon absorption (TPA) properties of the azulenylporphyrins and azulene-fused porphyrins have been comparatively studied by using DFT/B3LYP/6-31G(d) and the ZINDO/SDCI method. With the number of azulenyl groups increasing, the OPA wavelengths of all molecules are red-shifted in 400–600 nm and the two-photon absorption cross section is gradually enlarged. The azulene-fused structures facilitate an expanding conjugated area and increasing TPA cross section. The origin of TPA properties of studied compounds is studied with a two-level model. In summary, the azulene-fused porphyrins exhibit strong two-photon absorption.

Keywords: porphyrin, azulene, two-photon absorption
PACC: 4250

1. Introduction

Recently, materials with a large two-photon absorption cross section have found numerous applications in nonlinear optics, such as two-photon fluorescence excitation microscopy,[1] optical power limiting,[2] three-dimensional optical data storage,[3] two-photon up-conversion lasing,[4] photodynamic cancer therapy,[5] and so on. On all the above applications, the characteristics of two-photon absorption (TPA) are the transparency at low input light intensity, and the dependence of the absorption intensity on the square of the input light intensity.[6] Customary chromophores for nonlinear optics applications are based on design concepts that include strength of the electron donor and electron acceptor, and conjugation extension.[7−10] The architectural classes of TPA molecules have conventional linear structures, crosslinked polymers, banched polymers, helical oligomers, macrocycle molecular structures, and so on.[11]

Many recent studies focused on the TPA properties of porphyrins, which are suitable candidates for possible applications in nonlinear optics. It is well known that the monomeric metal-free porphyrins show a small TPA cross section $\delta(\omega)$ value, typically a ∼10 GM (1 GM=10^{50} $cm^4{\cdot}s{\cdot}photon^{-1}$). Hence, researchers have designed and synthesized porphyrin derivatives with a large TPA cross section value. One of the key design strategies to enhance the TPA cross-section $\delta(\omega)$ is to modify the porphyrin ring by incorporating different metal ions into the center of the porphyrin macrocycle or by linking different kinds of substituents to the peripheral positions of the porphyrin macrocycle.[12,13] Azulene is a resonance-stabilized nonalternant aromatic hydrocarbon. Its extraordinary photophysical property (the famous anomalous $S_2 \rightarrow S_0$ fluorescence) is discovered by Beer, Longuet and Higgins.[14] Based on an azulene unique π-system, a variety of functional dyes and nonlinear optical materials have been investigated.[15] Besides, azulene serves as either an electron donor or an electron acceptor, depending on the nature and connectivity of substituent.[16] Kurotobi *et al* have ex-

*Project supported by the National Natural Science Foundation of China and the Open Project of State Key Laboratory of Supramolecular Structure and Materials of Jilin University (Grant No SKLSSM200716).
†Corresponding author. E-mail: jikangf@yahoo.com

perimentally studied some properties of azulene-fused porphyrins[16,17]. In this paper, we mainly study the micro-essence of one- and two-photon absorption of azulenylporphyrin (PA series) and azulene-fused porphyrins (PFA series) comprehensively, and the relationship between the structure and the one- and two-photon absorption properties.

2. Computational methods

The TPA process corresponds to simultaneous absorption of two photons. The TPA efficiency of an organic molecule, at optical frequency $\omega/2\pi$, can be characterized by the TPA cross section $\delta(\omega)$. $\delta(\omega)$ relates to the imaginary part of the second hyperpolarizability $\gamma(-\omega;\,\omega,\,\omega,\,-\omega)$ by the following equation[18]

$$\delta(\omega) = \frac{3\hbar\omega^2}{2n^2c^2\varepsilon_0} L^4 \mathrm{Im}\left[\gamma\left(-\omega;\omega,\omega,-\omega\right)\right], \qquad (1)$$

in which $h\omega$ is the energy of the incoming photons, c is the speed of light, ε_0 is the vacuum electric permittivity, n denotes the refractive index of the medium and L corresponds to the local-field factor. In the calculations presented here, n, L are set to 1 (isolated molecule in vacuum).

The sum-over-states (SOS) expression to evaluate the components of the second hyperpolarizability $\gamma_{\alpha\beta\gamma\delta}$ can be induced out using the perturbation theory and density matrix method. By considering a Taylor expansion of energy with respect to the applied field, the $\gamma_{\alpha\beta\gamma\delta}$ Cartesian components are given by Refs.[19] and [20]. In the present work, all damping factors Γ are set to 0.14 eV, this choice of damping factor is found to be reasonable on the basis of the comparison between the theoretically calculated and experimental TPA spectra. To compare the calculated δ value with the experimental value measured in solution, the orientationally averaged (isotropic) value of γ is evaluated, which is defined as

$$\langle\gamma\rangle = \frac{1}{15}\sum_{i,j}\left(\gamma_{iijj} + \gamma_{ijij} + \gamma_{ijji}\right), \quad i,j = x,y,z, \quad (2)$$

substituting the imaginary part of $\langle\gamma\rangle$ value into the expression (1), $\delta\left(\omega\right)$, that can be comparable with the experimental value, is obtained.

In principle, any kind of self-consistent field molecular orbital procedure combined with configuration interaction can be used to calculate the physical values in the above expression. In this paper, the DFT/B3LYP/6-31G(d) method was first used to calculate molecular equilibrium geometries using the GAUSSIAN 03 program package.[21] Then, the property of electronic excited states was obtained by single and double electronic excitation configuration interaction (SDCI) using the ZINDO program.[22] It is well known that the original ZINDO algorithm by Zerner has been adapted only to single-CI, but one has to consider a double excitation configuration for correct determination of the third-order polarizability γ and two-photon absorption spectra; therefore, we added the double excitation configuration in ZINDO and restricted the CI-active spaces to the two highest occupied and two lowest unoccupied π-orbitals.[23] Then, a program (FTRNLO) compiled by our group is used to calculate the second hyperpolarizability γ and the TPA cross section according to formulas (1) and (2) and SOS formulas. Furthermore, the ground-state one-photon absorption spectra which are needed to predict the TPA properties of the molecule are provided.

3. Calculation results and discussion

3.1. Geometrical optimization and electronic structure

The investigated molecules (PA and PFA series) are shown in Fig.1. The molecules in the PA series are azulenlyporphyrins in which the 4-azulenyl group is directly linked to the porphyrin rings. Both PA2 and PA3 have atropisomers. PA2 includes PA2-1 and PA2-2, and PA3 includes PA3-1, PA3-2 and PA3-3 (shown in Fig.2). PFA series are azulene-fused porphyrins which are the product of a ring-closing reaction of the PA series. PFA2, which is the major product of PA2, is anti-isomer. When the terminal group is a 2, 4, 6-tert-butyl-phenyl group, PFA3 is the major product of PA3.[17] In order to save the calculating time and compare with other studied molecules conveniently, the 2, 4, 6-tert-butylphenyl is replaced by methyl groups. At the same time, the peripherally unsubstituted porphyrin nickel (II) (NiP) is chosen for reference and comparison.

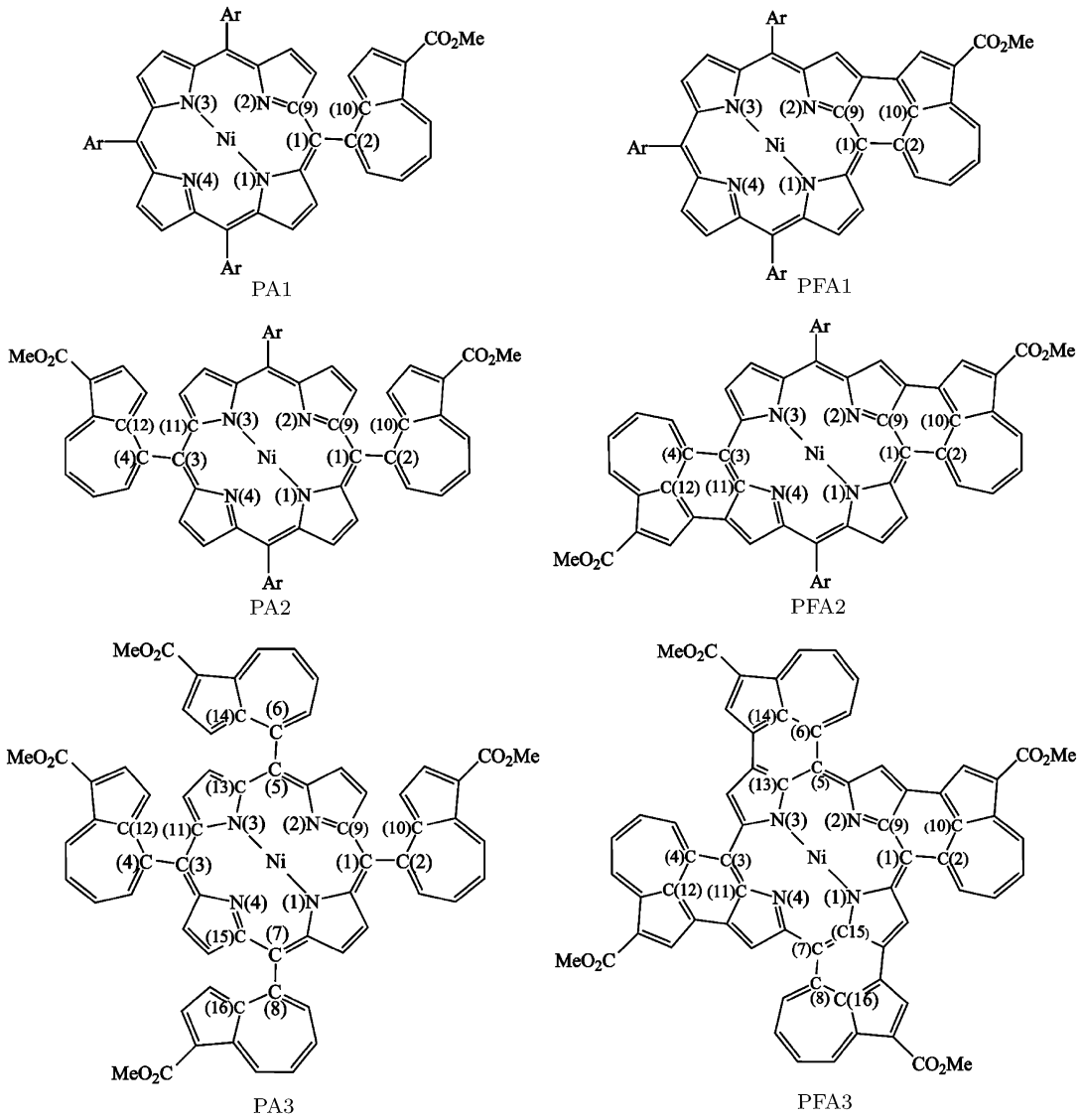


Fig.1. The investigated molecules and corresponding names and labels (Ar=phenyl).

All molecular geometries are optimized with a 6-31G(d) basis set at a density function theory B3LYP level. As shown in Table 1, each Ni-N bond length of NiP is 1.958 Å (1 Å=0.1 nm) which is only 0.001 Å bigger than that of Ref.[24] (1.957 Å). The relative error is 0.051%. For PA1, the C–C bond length which connects the 4-azulenyl group and porphyrin ring is 1.508 Å. It is similar to X-ray diffraction analysis (1.505 Å).[17] The relative error is 0.199%. Each Ni–N bond length of the optimal structure of PFA3 is 1.884 Å. The maximum error is 0.53% compared with the experimental data. A little deviation in value is due to the structure in vacuum which is more incompact than the crystal structure. Therefore, the DFT/B3LYP/6-31G(d) method in the GAUSSIAN 03 program package is suitable for our studied molecules. Adding azulenyl group(s) to NiP, the distance of Ni–N and N–N decreases in the PA and PFA series. However, with the increasing number of azulenyl groups, the average Ni–N lengths and the average N–N lengths are increased in PA series: PA1 (1.922 Å, 3.844 Å) < PA2-2 (1.923 Å, 3.846 Å) < PA2-1(1.925 Å, 3.850 Å) <PA3-2 (1.927 Å, 3.853 Å) <PA3-3 (1.928 Å, 3.855 Å) < PA3-1 (1.956 Å, 3.912 Å), and decreased in the PFA series: PFA1 (1.909 Å, 3.817 Å) > PFA2 (1.895 Å, 3.799 Å) > PFA3 (1.884 Å, 3.769 Å). It means the central porphyrin rings of molecules in the PA series are larger than the same part of relative molecules in the PFA series. For the PA series, the azulenyl groups are almost perpendicular to the porphyrin plane. For the PFA series, the central porphyrin is distored by fusing azulene moieties, and the azulene moieties and the porphyrin ring are approximately coplanar (shown

in Fig.2). The result shows that the PA series show the steric hindrance effect more obviously than the PFA series. As for atropisomers, cis-isomers have the largest central porphyrin ring. For example, cis form PA2-1 has a larger porphyrin ring than trans form PA2-2.

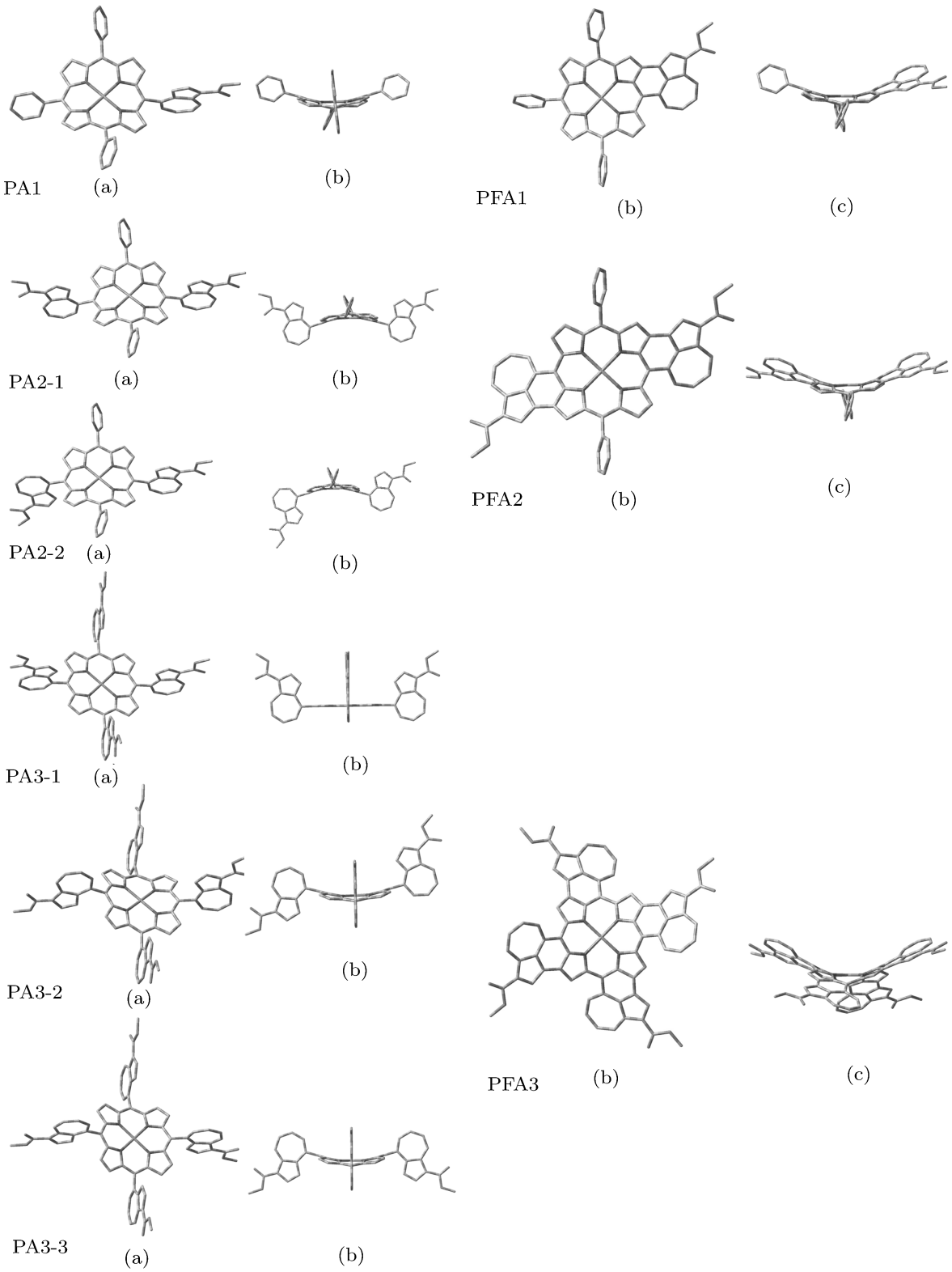


Fig.2. The equilibrium geometries of PA and PFA series. (a) Oblique view, (b) top view, and (c) side view. The hydrogen atoms have been omitted for clarity.

Table 1. Selected optimized bond length (Å) and dihedral angle (°) for the molecules.

	PA1	PA2-1	PA2-2	PA3-1	PA3-2	PA3-3	PFA1	PFA2	PFA3	(Exp.[a])	NiP(D_{4h})	(Exp.[b])
Ni–N(1)	1.920	1.923	1.921	1.956	1.927	1.927	1.916	1.908	1.884	(1.894)	1.958	(1.957)
Ni–N(2)	1.924	1.927	1.925	1.956	1.927	1.928	1.902	1.892	1.884	(1.863)	1.958	(1.957)
Ni–N(3)	1.921	1.923	1.921	1.956	1.927	1.927	1.909	1.908	1.884	(1.893)	1.958	(1.957)
Ni–N(4)	1.921	1.927	1.925	1.956	1.927	1.928	1.907	1.892	1.884	(1.877)	1.958	(1.957)
Ni(1)–Ni(3)	3.842	3.845	3.842	3.912	3.853	3.855	3.824	3.815	3.769		3.915	
Ni(3)–Ni(4)	3.845	3.854	3.850	3.912	3.853	3.855	3.809	3.783	3.769		3.915	
C(1)–C(2)	1.508	1.508	1.508	1.509	1.507	1.508	1.477	1.477	1.477			
C(3)–C(4)	N	1.508	1.507	1.509	1.508	1.508	N	1.477	1.477			
C(5)–C(6)	N	N	N	1.509	1.508	1.508	N	N	1.477			
C(7)–C(8)	N	N	N	1.509	1.508	1.508	N	N	1.476			
Φ(C(9)C(1)C(2)C(10))	91.31	88.66	88.92	89.75	93.07	–88.47	17.25	16.64	14.05			
Φ(C(11)C(3)C(4)C(12))	N	–87.60	97.61	–91.40	88.18	88.22	N	16.63	14.05			
Φ(C(13)C(5)C(6)C(14))	N	N	N	89.74	89.58	88.57	N	N	–13.89			
Φ(C(15)C(7)C(8)C(16))	N	N	N	–91.41	–89.59	–88.29	N	N	–14.07			

Note: Exp.[a] denotes Ref.[17]. Exp.[b] denotes Ref.[24]. N denotes no data.

The calculated frontier orbital energy data (4 occupied orbitals and 5 unoccupied orbitals) are listed in Table 2. The energy of HOMO (highest occupied molecular orbitals) increases when azulenylporphyrin is inverted to the ring-closing azulene-fused porphyrin, and at the same time the energy of LUMO (lowest unoccupied molecular orbitals) decreases. Meanwhile, the increasing numbers of the azulenyl groups do not affect the energy of HOMO and LUMO much. Compared with PA2-1 and PA2-2, the energy difference of HOMO (LUMO) is only 0.01 eV. For PA3-1, PA3-2 and PA3-3, the energy of HOMO and LUMO is the same (only the energy of LUMO of PA3-1 adds 0.01 eV). In other words, the electronic structures for atropisomers of PA2 (PA3) are almost the same. The HOMO-LUMO energy gaps ($\Delta E_{\mathrm{H-L}}$) sequence is as follows: PA1 2.91 (eV) > PA2-1 (2.90 eV) > PA2-2 (2.88 eV) > PA3-1 (2.82 eV) > PA3-2 (2.81 eV)=PA3-3 (2.81 eV), and PFA1 (2.10 eV) > PFA2 (1.70 eV) > PFA (1.46 eV). Herein, with identical numbers of azulenyl groups, PA series molecules have higher $\Delta E_{\mathrm{H-L}}$ than PFA series molecules. And increasing azulenyl groups is helpful to reduce $\Delta E_{\mathrm{H-L}}$. The reduction of the energy gap $\Delta E_{\mathrm{H-L}}$ normally brings on a bathochromic shift in the one-photon absorption spectra. Only considering the energy gap, we have presumed PFA3 the longest one-photon absorption wavelength and the most outstanding photophysical properties in all studied molecules.

Table 2. The B3LYP/6-31G(d) predicted molecular orbital energies of the studied compounds (unit: eV).

	HOMO-3	HOMO-2	HOMO-1	HOMO	LUMO	LUMO+1	LUMO+2	LUMO+3	LUMO+4
PA1	–5.79	–5.55	–5.17	–5.12	–2.21	–2.15	–2.03	–1.54	–0.92
PA2-1	–5.66	–5.55	–5.27	–5.19	–2.31	–2.25	–2.15	–2.06	–1.60
PA2-2	–5.65	–5.54	–5.27	–5.20	–2.30	–2.26	–2.13	–2.08	–1.60
PA3-1	–5.62	–5.61	–5.55	–5.28	–2.46	–2.46	–2.25	–2.20	–2.18
PA3-2	–5.63	–5.61	–5.51	–5.28	–2.47	–2.46	–2.24	–2.23	–2.18
PA3-3	–5.64	–5.62	–5.51	–5.28	–2.47	–2.47	–2.26	–2.23	–2.18
PFA1	–5.80	–5.48	–5.14	–4.82	–2.72	–2.15	–1.87	–1.40	–0.80
PFA2	–5.77	–5.25	–5.18	–4.74	–3.04	–2.30	–2.21	–1.92	–1.77
PFA3	–5.38	–5.30	–5.30	–4.61	–3.15	–3.15	–2.78	–2.16	–2.03

The origin of the Q and B bands in the electronic spectra of porphyrin derivatives is usually interpreted using the four-orbital model of M. Goutermann, which assumes that the HOMO and HOMO-1 are almost degenerate in energy and well separated from the other levels; a similar assumption is applicable to LUMO and LUMO+1.[13,25,26] From Table 2 and Fig.3, the four-orbital model approximately describes PA1 and PA2, because the other frontier orbitals are separated by a comparatively large energy gap between the two highest

HOMOs and lowest LUMOs. However, for other molecules studied here the four-orbital model is not applicable. So we anticipate that OPA spectra of PA1 will be blue-shifted compared with PA2.

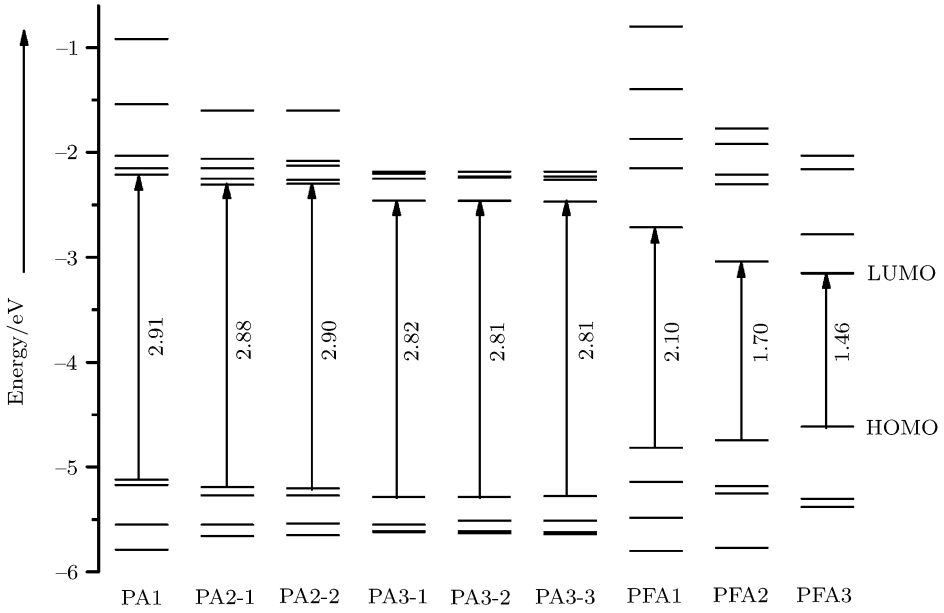


Fig.3. B3LYP/6-31G(d) predicted molecular orbital energy diagram of the studied compounds.

3.2. One-photon absorption

One-photon absorption properties of studied molecules calculated by using the ZINDO/SDCI method are summarized in Table 3, including the OPA wavelength (λ^{O}_{max}), the corresponding oscillator strength (f), and transition nature. The calculated TDDFT λ^{O}_{max} values of PFA1 and PFA2, and several experimental data are also given. As shown in Table 3, the calculated ZINDO/SDCI λ^{O}_{max} values are in good agreement with the experimental data. The differences between TDDFT and the experimental data are bigger than those between ZINDO and the experimental data. Therefore, a semiempirical ZINDO/SDCI method is appropriate for studied molecules in this work, and sometimes the results by the ZINDO/SDCI method are closer to the experimental data. To calculate the TPA properties, the first step is to accurately predict the OPA properties of the studied molecules. As seen in Table 3,

Table 3. The OPA properties for studied compounds.

mol.	λ^{O}_{max}/nm	f	transition nature	exp. data	mol.	λ^{O}_{max}/nm	f	transition nature	exp. data
PA1	444.1	0.08024	$S_0 \rightarrow S_6$	422	PFA1	526.6	0.03478	$S_0 \rightarrow S_3$	526(577.76[a])
	322.4	1.46661	$S_0 \rightarrow S_{15}$			447.8	0.11611	$S_0 \rightarrow S_8$	467
						375.3	0.88396	$S_0 \rightarrow S_{12}$	
PA2-1	444.3	0.18212	$S_0 \rightarrow S_4$	423	PFA2	747.2	0.45156	$S_0 \rightarrow S_1$	763(781.53[a])
	326.7	1.42223	$S_0 \rightarrow S_{13}$			530.2	0.07260	$S_0 \rightarrow S_5$	545
PA2-2	444.0	0.16470	$S_0 \rightarrow S_4$	423		465.8	0.27644	$S_0 \rightarrow S_8$	487
	326.8	1.56370	$S_0 \rightarrow S_{12}$			334.0	1.26136	$S_0 \rightarrow S_{22}$	
PA3-1	445.4	0.15395	$S_0 \rightarrow S_4$	437	PFA3	580.9	0.04022	$S_0 \rightarrow S_7$	574
			$(S_0 \rightarrow S_{5)}$			368.3	0.56634	$S_0 \rightarrow S_{27}$	
	320.2	0.97140	$S_0 \rightarrow S_{20}$						
PA3-2	445.4	0.17133	$S_0 \rightarrow S_4$	437	NiP	628.9	0.03846	$S_0 \rightarrow S_1$	628.9[b]
	318.2	0.98991	$S_0 \rightarrow S_{22}$						(623.7)[c]
PA3-3	444.3	0.17231	$S_0 \rightarrow S_4$	437		355.5	1.14596	$S_0 \rightarrow S_{12}$	352.1
	318.2	0.94421	$S_0 \rightarrow S_{21}$						(336.9)[c]

Note: exp. data denotes Ref.[17] and the supporting information of Ref.[17].

a denotes the TDDFT/6-31G(d) results. b and c denote Refs.[25] and [29], respectively.

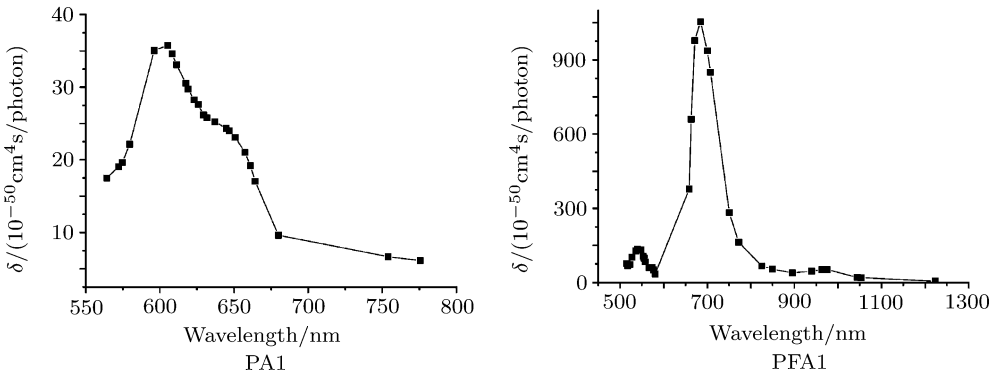
λ^{O}_{max} with the largest oscillator strength of PFA series exhibit a bathochromic shift compared with that of the PA series, when the two series have equal numbers of azulenyl groups. In 400–600 nm, the OPA wavelength of the PFA series molecules is red-shifted with the increasing number of azulenyl groups. The PA series present the same tendency. In this paper, electron structures cannot predict OPA properties well. Because the transition from HOMO to LUMO is not an important part for the OPA final state, the HOMO–LUMO energy gap cannot predict one-photon absorption wavelength. In addition, for all studied molecules, the calculated λ^{O}_{max} with the largest oscillator strength are all in the UV region, therefore, azulenylporphyrins and azulene-fused porphyrins possess good transparency which is important for optical power limiting (OPL) applications.

3.3. Two-photon absorption

According to expressions (1) and (2), we compiled a program to calculate the third-order polarizability $\gamma_{\alpha\beta\gamma\delta}$ and the TPA cross section δ_{max}. Figure 4 shows two-photon absorption spectra in the incident light wavelength range from 600 nm to 800 nm, in order to provide a more obvious comparison for studied molecules in this work. Table 4 summarizes the TPA maximum absorption wavelength λ^{T}_{max}, transition nature, maximum TPA cross section δ^{T}_{max}, and main configuration coefficient and weights. A good TPA material means it is made up of the molecule with a large δ^{T}_{max} value. For the PA and PFA series, the δ^{T}_{max} values increase with the increasing azulenyl groups. Herein, as shown in Fig.4 the δ^{T}_{max} values of PA2 molecules are 56.97 GM (PA2-1) and 47.79 GM (PA2-2), respectively. The δ^{T}_{max} value of PA3-1 (68.91 GM) is the largest in PA3 molecules. The phenomenon shows that the cis-form structures of PA2 and PA3 show good TPA cross-section values. The maximum TPA cross section of molecules of the PFA series is much bigger than that of the corresponding molecules of the PA series, at the same time, the λ^{T}_{max} values are a bathochromic shift. The azulene-fused structures facilitate the expanding conjugated area and increasing TPA cross section.

Table 4. The TPA properties for studied molecules. H, H–n L and L+n denote HOMO, HOMO–n, LUMO and LUMO+n, respectively.

mol.	λ^{T}_{max}/nm	transition nature	δ^{T}_{max}/GM	main configuration coefficient and weights
PA1	605.2	$S_0 \rightarrow S_{26}$	35.75	–0.67(H–2,H–1→L+1,L+2)–0.39(H–2,H–1→L+1,L+2(1))
PA2-1	613.0	$S_0 \rightarrow S_{25}$	56.97	–0.82(H–3→L)–0.35(H–3→L+1)
PA2-2	617.4	$S_0 \rightarrow S_{24}$	47.79	0.33(H–1,H→L,L)–0.49(H–1,H→L,L+1)+0.37(H,H→L,L)–0.41 (H,H→L+1,L+1)
PA3-1	613.4	$S_0 \rightarrow S_{31}$	68.91	0.93(H–1→L+3)
PA3-2	613.8	$S_0 \rightarrow S_{34}$	68.82	0.59(H–1→L+2)–0.57(H–1→L+5)+0.37(H–1→L+11)
PA3-3	611.4	$S_0 \rightarrow S_{35}$	63.39	–0.33(H–1→L+12)+0.53(H–1,H→L,L+1)–0.36(H,H→L,L+1)
PFA1	684.4	$S_0 \rightarrow S_{15}$	1053.76	–0.44(H–2→L+1)+0.33(H–1,H→L,L+1)
PFA2	633.4	$S_0 \rightarrow S_{29}$	1136.64	–0.34(H–1→L+7)+0.36(H–1,H–1→L,L)
PFA3	668.6	$S_0 \rightarrow S_{40}$	1184.47	–0.76(H–1→L+4)



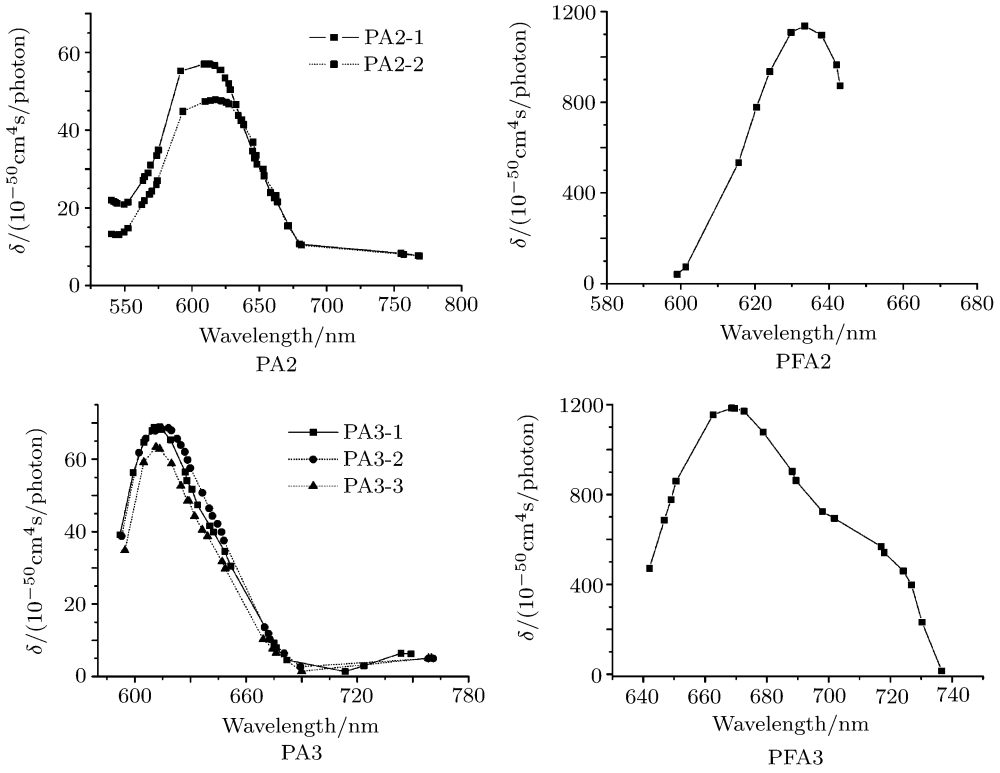


Fig.4. Two-photon absorption spectra.

In order to explain the origin of TPA properties of the investigated molecules, we used a two-level model, in which the TPA cross section can be defined as[27,28]

$$\delta = \frac{4\pi^2 a_0^5 \alpha\omega^2}{15c_0} \frac{M_{0n}^2 \Delta\mu_{0n}^2}{E_{0n}^2 \Gamma}, \tag{3}$$

where a_0 is the Bohr radius, c_0 is the speed of the light, α is the fine structure constant, ω is the photon energy, M_{0n} is the transition dipoles between the ground state $|0\rangle$ and a TPA final state $|n\rangle$. $\Delta\mu_{0n}$ is the dipole moment difference between ground and excited states, E_{0n} is the transition energy between the ground states $|0\rangle$ and a TPA final state $|n\rangle$. The formula (3) can be simplified to the following formula

$$\delta \propto \frac{M_{0n}^2 \Delta\mu_{0n}^2}{E_{0n}^2 \Gamma}. \tag{4}$$

In this paper, the two-photon absorption cross sections of PA2-1 and PA3-1 are larger than other corresponding atropisomers. Therefore, we focus on the cis-isomers in the following discussion. Table 5 lists data and parameters of formula (4). In the PA series and PFA series molecules, the results of formula (4) show the same increasing trend with the $\delta_{\max}^{\mathrm{T}}$ values. In the PA (PFA) series, PA2-1 (PFA2) has the largest M_{0n} value; PA3-1 (PFA3) has the highest $\Delta\mu_{0n}$ value, at the same time, PA3-1 (PFA3) also has the largest calculated value of formula (4). In a word, $\Delta\mu_{0n}$ plays an important role in increasing the maximum TPA cross section.

Table 5. Data and parameters of two-level model for studied molecules.

	PA1	PFA1	PA2-1	PFA2	PA3-1	PFA3
M_{0n}^2/Debye	2.412	2.407	21.663	10.189	0.0161	8.196
$\Delta\mu_{0n}^2$/Debye	0.006	14.234	0.001	4.339	2.267	36.222
E_{0n}/eV	4.097	3.623	4.045	3.937	4.043	3.709
X	0.006	18.638	0.009	20.377	0.061	154.142
$\delta_{\max}$/GM	35.75	1053.76	56.97	1136.64	68.91	1184.47

$X = \frac{M_{0n}^2 \Delta\mu_{0n}^2}{E_{0n}^2 \Gamma}$

By comparing the PFA series molecules with the corresponding PA series molecules, we draw several conclusions as follows: (i) A visible increase of $\Delta\mu_{0n}$ takes the main responsibility for increasing the $\delta_{\max}$ value; (ii) The transition energy E_{0n} becomes smaller; (iii) For PA3-1 and PFA3, the difference of M_{0n} is also the main reason for the increasing two-photon absorption cross section. Charge transfer could interpret the increase of the TPA cross section. Here, we analyzed the charge transfer in the TPA processes of PA3-1 and PFA3. In Table 4, as to molecule PA3-1, the TPA transition nature is $S_0 \rightarrow S_{26}$ and the main configuration is HOMO-1→LUMO+3. In the case of PFA3, the TPA is produced by $S_0 \rightarrow S_{40}$, to which the configuration HOMO-1→LUMO+4 makes the main contributions.

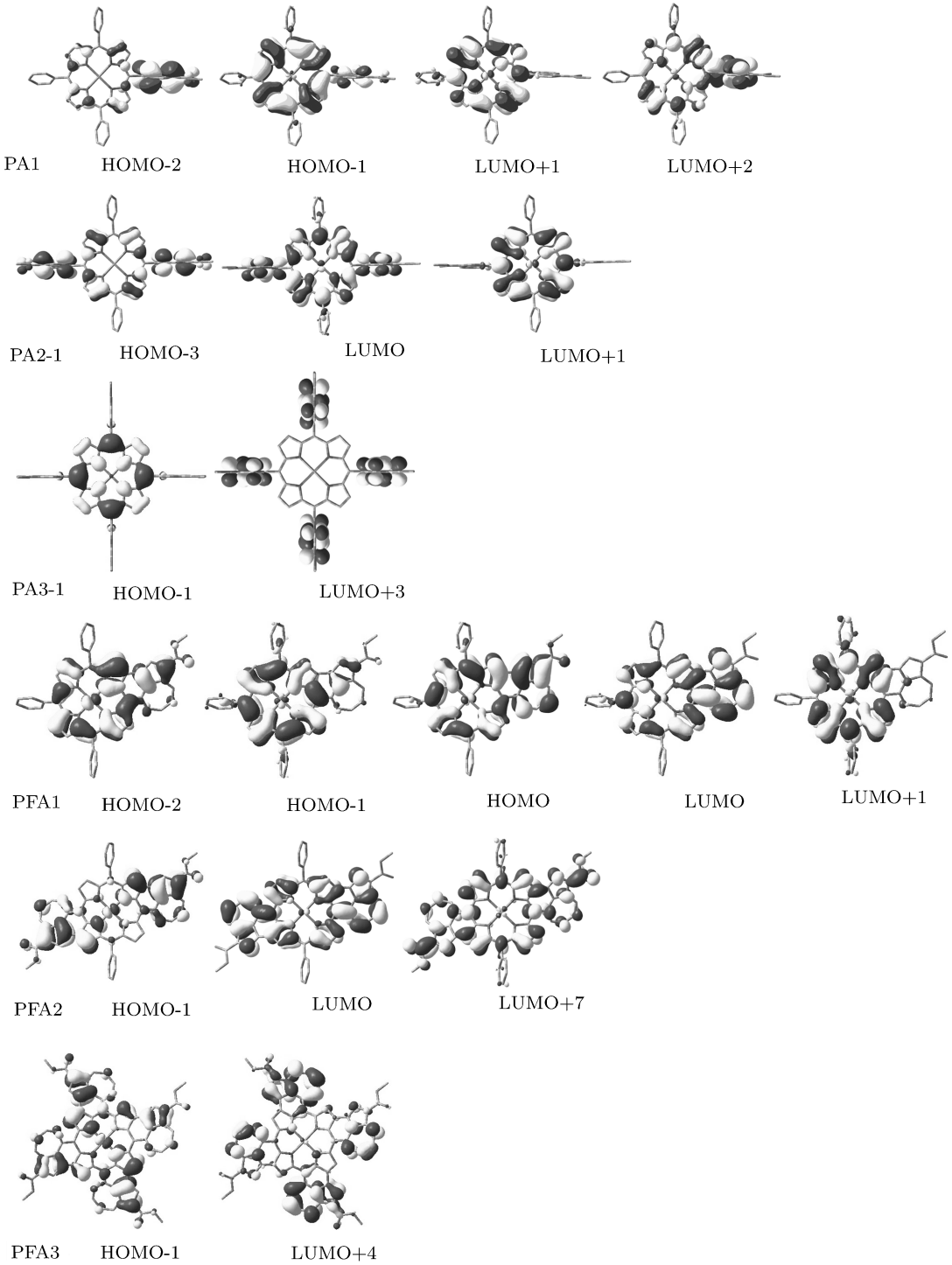


Fig.5. Contour surfaces of the frontier orbitals concerning the maximum two-photon absorptions for PA1, PA2-1, PA3-1, PFA1, PFA2 and PFA3. The hydrogen atoms have been omitted for clarity.

Contour surfaces of the frontier orbitals related to the TPA properties of studied molecules are plotted in Fig.5. For PA3-1, the molecular orbital of HOMO-1 mostly concentrates on the central porphyrin ring while the molecular orbital of LUMO+3 mostly locates in four azulene moieties. Therefore, intermolecular charge transfer goes from the central porphyrin ring to four azulene moieties. PA3-1 has obvious intermolecular charge transfer among the PA series. For PFA3, the molecular orbital of HOMO-1 distributes the whole molecule, the molecular orbital of LUMO+4 is mainly located in the periphery of the molecular structure, so intermolecular charge transfers from the whole molecule to the periphery of the molecule. As to the molecule orbital of HOMO-1, PFA3 has better π conjugation than PA3-1. Even for the TPA final state of PFA3 and PA3-1, PFA 3 exhibits a small conjugate phenomenon. As seen in Table 2, for PA3, the energy gap between HOMO-1 and LUMO+3 is 3.08 eV; for PFA3, the energy gap between HOMO-1 and LUMO+4 is 2.58 eV. Intermolecular charge transfer of PFA3 occurs more easily compared with PA3-1 in the TPA processes.

4. Conclusion

In this paper, the molecular geometries, electronic structures, and one- and two-photon absorption properties of the PA series and PFA series have been theoretically investigated with DF/B3LYP/6-31G(d) associated with the ZINDO/SDCI method. Our calculations show that the structure of azulene-fused and the number of azulenyl groups influence one- and two-photon absorption properties. With the number of azulenyl groups increasing, the TPA cross-section values are increased in the PA series (35.75 GM (PA1) $<$ 47.79 GM (PA2-2) $<$ 56.97 GM (PA2-1) $<$ 63.39 GM (PA3-3) $<$ 68.82 GM (PA3-2) $<$ 68.91 GM (PA3-1)) and in PFA series (1053.76 GM (PFA1) $<$ 1136.64 GM (PFA2) $<$ 1184.47 GM (PFA3)). Building a molecular frame like the PFA series possesses a large value of TPA cross section. The calculated $\lambda_{\max}^{\mathrm{O}}$ with the largest oscillator strength of studied molecules are all in the UV region. PFA series molecules in this work are promising candidates for TPA materials exhibiting strong two-photon absorption.

References

[1] Kohler R H, Cao J, Zipfel W R, Webb W W and Hansen M R 1997 *Science* **276** 2039

[2] Bhawalkar J D, He G S and Prasad P N 1995 *Opt. Commun.* **119** 587

[3] Strickler J H and Webb W W 1993 *Adv. Mater.* **5** 479

[4] Zheng Q, He G S, Lin T C and Prasad P N 2003 *J. Mater. Chem.* **13** 2499

[5] Bhawalkar J D, Kumar N D, Zhao C F and Prasad P N 1997 *J. Clin. Laser Med. Surg.* **15** 201

[6] Abbotto A, Beverina L, Bozio R, Bradamante S, Ferrante C, Pagani G A and Signorini R 2000 *Adv. Mater.* **12** 24

[7] Verbiest T, Houbrechts S, Kauranen M, Clays K and Persoons A 1997 *J. Mater. Chem.* **7** 2175

[8] Marder S R, Kippelen B, Jen A K Y and Peyghammbarian N 1997 *Nature* (London) **388** 845

[9] Dalton L R, Steier W H, Robinson B H, Zhang C, Ren A, Garner S, Chen A, Londergan T, Irwin L, Carlson B, Fifield L, Phelan G, Kincaid C, Amend J and Jen A 1999 *J. Mater. Chem.* **9** 1905

[10] Wolff J J and Wortmann R 1999 *Adv. Phys. Org. Chem.* **32** 121

[11] Ma H and Jen A K Y 2001 *Adv. Mater.* **13** 15

[12] Zhang X B, Feng J K, Ren A M and Sun C C 2006 *J. Mol. Struct.: THEOCHEM* **767** 165
Zhou X, Ren A M and Feng J K 2004 *Chem. Eur. J.* **10** 5623
Zhou X, Ren A M, Feng J K, Liu X J and Zhang Y D 2003 *Chem. Phys. Chem.* **4** 991
Yang Z D, Feng J K, Ren A M and Sun C C 2006 *J. Phys. Chem.* A **110** 13956
Liu X J, Feng J K, Ren A M, Cheng H and Zhou X 2004 *J. Chem. Phys.* **121** 8253

[13] Gouterman M 1978 in *The Porphyrins* Vol. III, ed. Dolphin D (New York: Academic) p1
Huang W T, Li Y, Xiang H, Yang H, Gong Q H, Huang Y Y, Huang C H and Jiang J Z 2005 *Chin. Phys.* **14** 2226
Chen Z F, Huang J W, Ji L N, Liu J, Shen H, Shen Y and Wang H 2008 *Acta Phys. Sin.* **57** 7354 (in Chinese)

[14] Beer M B, Longuet È and Higgins H C 1995 *J. Chem. Phys.* **23** 1390

[15] Woodford J N, Wang C H, Asato A E and Liu R S H 1999 *J. Chem. Phys.* **111** 4621

[16] Kurotobi K and Osuka S 2005 *Org. Lett.* **7** 1055

[17] Kurotobi K, Kim K S, Noh S B, Kim D and Osuka A 2006 *Angew. Chem. Int. Ed.* **45** 3944

[18] Cavlor C L, Dobrianow I, Kimmer C, Thome R E, Zipfel W and Webb W W 1999 *Phys. Rev.* E **59** 3831

[19] Orr B J and Ward J F 1971 *Mol. Phys.* **20** 513

[20] Dick B, Hochstrasser R M and Trommsdorff H P 1987 *Nonlinear Optical Properties of Organic Molecules and Crystals* (Orlando, FL: Academic) p167

[21] Frisch M J, Trucks G W Schlegel H B, Scuseria G E, Robb M A, Cheeseman J R, Montgomery J A Jr, Vreven T, Kudin K N, Burant J C, Millam J M, Iyengar S S, Tomasi J, Barone V, Mennucci B, Cossi M, Scalmani G, Rega N, Petersson G A, Nakatsuji H Hada M, Ehara M, Toyota K, Fukuda R, Hasegawa J, Ishida M, Nakajima T, Honda Y, Kitao O, Nakai H, Klene M, Li X, Knox J E,

Hratchian H P, Cross J B, Adamo C, Jaramillo J, Gomperts R, Stratmann R E, Yazyev O, Austin A J, Cammi R, Pomelli C, Ochterski J W, Ayala P Y, Morokuma K, Voth G A, Salvador P, Dannenberg J J, Zakrzewski V G, Dapprich S, Daniels A D, Strain M C, Farkas O, Malick D K, Rabuck A D, Raghavachari K, Foresman J B, Ortiz J V, Cui Q, Baboul A G, Clifford S, Cioslowski J, Stefanov B B, Liu G, Liashenko A, Piskorz P, Komaromi I, Martin R L, Fox D J, Keith T, Al-Laham M A, Peng C Y, Nanayakkara A, Challacombe M, Gill P M W, Johnson B, Chen W, Wong M W, Gonzalez C and Pople J A 2004 *GAUSSIAN 03* Revision C02, Gaussian, Inc Wallingford CT

[22] Anderson W P, Edwards W D and Zerner M C 1986 *Inorg. Chem.* **25** 2728

[23] Zhou X, Feng J K and Ren A M 2004 *Chem. Phys. Lett.* **397** 500

Zhang X B, Feng J K, Ren A M and Sun C C 2006 *J. Phys. Chem.* A **110** 12222

Zhang X B, Feng J K and Ren A M 2007 *J. Phys. Chem.* A **111** 1328

Coe B J, Samoc M, Samoc A, Zhu L, Yi Y and Shuai Z 2007 *J. Phys. Chem.* A **11** 472

[24] Flescher E B, Miller C K and Webb L E 1964 *J. Am. Chem. Soc.* **86** 2342

[25] Edwards L, Dolphin D H and Gouterman M 1970 *J. Mol. Spect.* **35** 90

[26] Spellane P J, Gouterman M, Antipas A, Kim S and Liu Y C 1980 *Inorg. Chem.* **19** 386

[27] Luo Y, Oscar R P, Guo J D and Agren H 2005 *J. Chem. Phys.* **455** 96101

[28] Oscar R P and Agren H 2006 *J. Chem. Phys.* **124** 094310

[29] Feng J K, Gao X L, Hao H S and Sun C C 1992 *Acta Chim. Sin.* **50** 874 (in Chinese)